Graphical Table of Contents

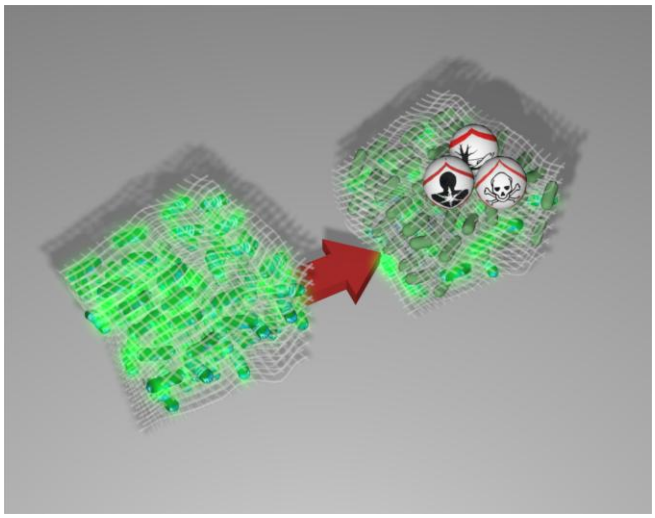

A composite material based on bacterial nanocellulose operating as both a culture scaffold and a biosensing substrate and luminescent bacteria *Aliivibrio fischeri* operating as a bio-indicator is reported. This nanobiocomposite is utilized as a simple-to-fabricate and user-friendly device for toxicity detection via determination of the bioluminescent inhibition caused by the exposure to various contaminants.

Bioluminescent Nanopaper for the Fast Screening of Toxic Substances

Jie Liu, Eden Morales-Narváez, Jahir Orozco, Teresa Vicent, Guohua Zhong*, Arben Merkoçi*

Bioluminescent Nanopaper for the Fast Screening of Toxic Substances

Jie Liu[1, 2], Eden Morales-Narváez[1], Jahir Orozco[1], Teresa Vicent[3], Guo-Hua Zhong[2] and Arben Merkoçi[1, 4*]*

[1] Catalan Institute of Nanoscience and Nanotechnology (ICN2), CSIC and the Barcelona Institute of Science and Technology, Campus UAB, Bellaterra, 08193 Barcelona, Spain

[2] Laboratory of Insect Toxicology, Key Laboratory of Pesticide and Chemical Biology, Ministry of Education, South China Agricultural University, Guangzhou 510642, P. R. China

[3] Departament d'Enginyeria Química, UniversitatAutònoma de Barcelona, Bellaterra Barcelona 08193, Spain

[4] Institucio Catalana de Recerca i Estudis Avançats (ICREA), Barcelona 08010, Spain

*guohuazhong@scau.edu.cn

*arben.merkoci@icn2.cat

Abstract: Environmental pollution is threatening human health and ecosystems as a result of modern agriculture techniques and industrial progress. A simple nanopaper-based platform coupled with luminescent bacteria *Aliivibrio fischeri* (*A. fischeri*) as a bio-indicator is presented for the rapid and sensitive toxicity evaluation of contaminants. When exposing to toxicants, the light inhibition on *A. fischeri*–decorated bioluminescent nanopaper (BLN) can be quantified and analyzed to classify the toxic level of a pollutant. The BLN composite was characterized in terms of morphology and functionality. Given the outstanding biocompatibility of nanocellulose in bacteria proliferation, BLN achieved high sensitivity with low cost and simplified procedure compared to a conventional instrument for lab use only. The broad applicability of BLN devices upon environmental samples was studied in spiked real matrix (lake and sea water), and their potential for the direct and *in-situ* toxicity screening was demonstrated. The BLN architecture can not only survive but also maintain its function during freezing storage and recycling process, which endowed BLN system with competitive advantages as a deliverable, ready-to-use device in large-scale manufacturing. The novel luminescent bacteria-immobilized nanocelullose-based device shows outstanding capabilities for toxicity bioassay of hazardous compounds, bringing new possibilities for cheap and efficient environmental monitoring of potential contamination.

Keywords: bacterial nanocellulose, nanopaper, *Aliivibrio fischeri*, bioluminescent device, toxicity bioassay

Introduction

Along with the great benefits from modern agricultural and industrial development, it has been attracting more and more attention over the environmental pollution that originating from human activities. Conventional techniques such as gas or liquid chromatography, dissolved oxygen content and chemical oxygen demand have been widely applied to characterize toxic compounds [1-5]. However, these techniques only indicate the nature (structure and composition) of the pollutants, but their biological effect on live organisms is also important to investigate [6]. Therefore, a range of toxicity bioassays that involves various organisms (e.g., plants, aquatic invertebrate, fish, algae and microorganisms) have been developed by taking advantages of the biological response of live organisms against contaminants [7-11]. Particularly, many microorganism species have been selected because of their ecological importance and physiological diversity [8, 11]. In 1978, the commercially available, ready-to-use kit Microtox® assay was developed based on luminescent marine bacterium *Aliivibrio fischeri* (*A. fischeri*) as a bio-indicator to determine the toxicity of environmental samples [6, 9]. *A. fischeri* can emit blue-green light during its metabolism, which could be inhibited when exposing to toxic substances. By measuring the light inhibition, the toxicity can be converted as EC_{50}, which expresses the concentration of toxicant corresponding to a 50% inhibitory effect. So far, Microtox® test has shown broad sensitivity and applicability to more than 2,700 different pollutants of interest [12-16].

Due to its high cost and unique analytical equipment, the Microtox® kit may lack the ability of large-scale *in-situ* screening. An alternative based on immobilized bacteria may provide a feasible scheme to perform low-cost and simple-to-operate detection of hazardous compounds as well as maintain highly functional bacteria [17-20]. In this process, the material used as substrate is crucial because of its dramatic effects on the survival and function of the immobilized bacteria.

Recently, bacterial cellulose nanopaper produced by *Acetobacter xylinum* has shown up excellent potential in several fields [21-23]. Thanks to its remarkable physical properties, special surface chemistry and excellent biological properties (biocompatibility and biodegradability), bacterial cellulose nanopaper has been selected as a culture skeleton for the cell proliferation [24-25] which suggest its potential to be a desirable substrate for bioluminescent *A. fischeri*.

Herein, we present a cheap, sensitive, efficient and robust platform for toxicity bioassay based on bioluminescent nanopaper (BLN) devices consisting of bacteria as a bio-indicator and bacterial nanocellulose as bio-scaffold (see **Scheme 1**). While *A. fischeri* immobilized on nanopaper is exposed to a toxicant, the bioluminescence is efficiently inhibited as a toxicity indicator in a short time (5 to 15 minutes). Firstly, *A. fischeri* was immobilized into the fiber networks of nanocellulose to form the BLN composite. The as-prepared nanopaper devices were characterized in terms of their morphology and function. The fact of having luminescent bacteria fully distributed in a cheap and green bio-substrate offers the possibility of a rapid toxicity evaluation of a myriad of toxic compounds. Diuron, tributyltin (TBT) and polybrominated diphenyl ether (PBDE) were chosen as typical contaminants that sensitively induced the bioluminescence inhibition of BLN to varying degrees. The sensitivity and applicability of BLN upon real matrix were also determined. Through frozen storage and recycling process, the BLN architectures exhibited competitive advantages as robust, deliverable and ready-to-use devices. The BLN-based bioassay demonstrated outstanding capabilities for toxicity evaluation with a miniaturized setup and flexible procedure, which brings innovative possibilities for general toxicity screening and environmental monitoring.

1. Materials and methods

1.1 Reagents and equipment

Bacterial cellulose nanopaper was purchased from Nanonovin Polymer Co. (Mazandaran, Iran). Diuron (98%), tributyltin chloride (96%), acetonitrile, ethanol, sodium chloride, tryptone, sea salts, yeast extract, sucrose, glycine and glycerol (99%) were purchased from Sigma-Aldrich (Taufkirchen, Germany). Stock solutions of diuron (10 g L^{-1}) and TBT (1 mM) were prepared in acetonitrile and ethanol, respectively and stored at 4 °C. Polybrominated diphenyl ether (PBDE) (1 mg L^{-1}) was purchased from AccuStandard Inc (New Haven, CT, USA). Cellulose membrane CFSP001700 was acquired from Millipore (Billerica, MA, USA). Scanning electron microscopy (SEM) imaging was performed through a Magellan 400L SEM High Resolution SEM (FEI, Hillsboro, OR, USA). Photoluminescence images were obtained using a Typhoon 9410 Variable Mode Imager (GE, Freiburg, Germany). Confocal imaging was performed using a SP5 confocal microscope (Leica, Wetzlar, Germany). Bioluminescence intensity was estimated using ImageJ 1.46r (Wayne Rasband, National Institutes of Health, Bethesda, MD, USA). The optical density of bacteria was measured by Perkin Elmer Victor3 Multilabel Plate Counter (Waltham, MA, USA). Microtox® assay was performed on a Microtox® M500 toxicity analyser (Modern Water, New Castle, DE, USA). Lake water samples were collected from Sant Cugat Lake (Barcelona, Spain). Seawater samples were extracted from Masnou Beach (Barcelona, Spain). Lake water and seawater samples were filtered using filter paper and then a nitrocellulose membrane (0.025 μm, Millipore, Billerica, Massachusetts, USA) prior to use.

1.2 The cultivation of A. fischeri and its bioluminescence emission

A. fischeri was isolated from Microtox® reagent by aseptically adding 1 mL of reconstruction solution to a microbial reagent vial and then inoculating the homogenized solution on a marine agar plate. After 24 h, the sole colony emitting bioluminescence was picked up by sterilized loop and inoculated into 50 mL of marine broth in a 250-mL Erlenmeyer flask placed on an

incubation shaker at 25 ℃, 140 rpm. The modified marine broth (MB) [26] contained tryptone (5 g L^{-1}), yeast extract (3 g L^{-1}), glycerol (3 mL L^{-1}) and sea salts (40 g L^{-1}). To prepare the solid marine agar (MA) plate, 15 g L^{-1} of agar powder was added in marine broth. Both media were sterilized at 121 ℃ for 20 min and cooled/fused to room temperature prior to use.

A. fischeri was respectively inoculated to three substrates: MA, MB and sterile nanocellulose pieces (5mm of diameter, round-shaped pieces). To prepare sufficient nutrient for bacteria multiplication, nanocellulose was previously immersed in marine broth for nutrient adsorption for 2 h. 1 μL of bacteria suspension at 1.2 of optical density (OD_{600nm}), which was around 2.3×10^8 of colony-forming units (CFU) mL^{-1}, was inoculated in 100 μL of marine broth/agar or one piece of nanopaper in the individual well of 96-well microplate. 9 replicates and three blanks were settled for each substrate. The OD_{600nm} and luminescent intensity were respectively measured through a microplate reader and a Typhoon 9410 scanner every 2 h within 24 h to determine the growth and bioluminescence tendency among three groups.

Additionally, the procedure for routine cultivation was performed as follows. 50 μL of bacterial suspension at 1.2 of OD_{600nm} (2.3×10^8 CFU mL^{-1}) was inoculated in 50 mL of MB in a 250-mL Erlenmeyer flask and incubated on a shaker at 25 ℃, 140 rpm.

1.3 The preparation of BLN and its morphological observation

In order to obtain BLN samples emitting homogeneous bioluminescence, the sterilized nanocellulose pieces were added into 50 mL of MB in a 250-mL Erlenmeyer flask with 0.1% of inoculum. After 18 h of incubation, the BLN pieces were individually placed into the wells of 96-well microplate prior to observation. The appearances of bare nanopaper and BLN were separately captured by iPhone 6.0 (Apple Inc, Cupertino, CA, USA) and Typhoon 9410 scanner

145 to analyze their physical and luminescent images. The composites ready for SEM imaging were
146 prepared according to a published method without final sputtering of gold [27]. Briefly, bare
147 nanopaper and BLN pieces were dehydrated by gradient elution using ethanol and
148 hexamethyldisilazane (HMDS) for the critical point drying. As for the confocal microscopy, the
149 BLN composites were stained by the mixture of 4 μL of Hoechst 33342 (Molecular Probe Inc,
150 Eugene, OR, USA) and 500 μL of phosphate-buffered saline for 15 min prior to imaging.

151 1.4 Toxicity assay using Microtox®

152 Microtox® reagents were supplied by Modern Water (New Castle, DE, USA) as freeze-dried
153 powder batches and stored at -20°C prior to use. The toxicity analysis of three contaminants,
154 diuron (100 mg L^{-1}), TBT (0.1 mM) and PBDE (1 mg L^{-1}), were conducted respectively
155 according to Microtox® protocol (AZUR Environmental, New Castle, DE, 1998). Briefly, the
156 serial dilutions of the target compound were individually mixed with the same volume of
157 reconstructed reagents. The inhibition of bioluminescence was measured by M500 luminescent
158 analyser after exposure 5 and 15 min and expressed as the EC_{50} values.

159 1.5 Toxicity assay using bioluminescent bacterial suspension

160 After 18 h of routine cultivation, *A. fischeri* was collected by centrifugation at 6000 rpm for 10
161 min, washed twice and suspended in 10 mL of 2% NaCl. 100 μL of bacterial suspension was
162 first added by a multichannel pipette to each well of a 96-well microplate. 1:2 serial dilutions of
163 diuron, TBT and PBDE were performed by transferring 1 mL sample into 1 mL of 2% NaCl and
164 mixed after each transfer. 100 μL of each diuron/PBDE (or 50 μL of TBT) dilutions were added
165 into the well containing 100 μL of bacterial suspension and mixed. Three replications were
166 prepared and the treatments without toxic compounds were carried out as control. After exposure

for 5 and 15 min, the bioluminescence intensity in microplates was scanned by a Typhoon 9410 scanner and analyzed through ImageJ 1.46r.

1.6 Toxicity assay using bacteria-decorated BLN

The BLN pieces with homogeneous luminescence were prepared as described previously. After 18 h of cultivation, bacteria-decorated BLN composites were collected and placed individually in each well of a 96-well microplate. 1:2 serial dilutions of diuron, TBT and PBDE were performed as described. Each BLN piece was mixed with 100 μL of each diuron/PBDE (or 50 μL of TBT) dilutions. The mixtures without toxic compounds were carried out as blank controls. After exposing 5 and 15 min, the bioluminescence intensity in microplates was scanned by a Typhoon 9410 scanner and analyzed via ImageJ 1.46r.

1.7 Toxicity assay in real matrixes

To explore the applicability of BLN devices upon real matrix, toxicity bioassay using BLN was performed in both lake water and seawater systems. Likewise, the evaluation by bacterial suspension was designed as a comparison group. The stock solutions of diuron, TBT and PBDE were blended in lake/sea water to reach working concentrations. 1:2 serial dilutions of target compounds were prepared by transferring 1 mL sample into 1 mL of lake/sea water and mixing after each transfer. Then the bioassay using bacterial suspension or BLN pieces were conducted as described before. The bioluminescent images were collected by a Typhoon 9410 scanner and analyzed using ImageJ 1.46r.

1.8 Frozen-thawed process

An easy-to-operate frozen-thawed strategy was adopted to realize the storage of BLN platform. Basically, the biomaterials are frozen under the protection of reagents such as polyalcohols, amino acids and disaccharides and thawed to normal status prior to use. The recovered biomaterials are expected to maintain viable or normal function after a frozen-thawed process. In this case, three general protective agents (sucrose, glycine and glycerol) were employed to select the most suitable protectant for the frozen-thawed process of BLN. Specifically, each protectant was prepared as 1%, 3%, 5%, 10% and 15% solutions with Milli-Q water and sterilized at 121 ℃ for 20 min. BLN pieces were placed individually in a 96-well microplate and the luminescent intensity was scanned and recorded as the initial intensity. 50 μL of protectant solution was mixed with single BLN piece and three replicates were performed in each concentration. The bioluminescence intensity was recorded as ¨adding protectant¨ before freezing at -20 ℃. After freezing for 2 h, the composites were thawed and the luminescence at ¨just-thawed¨ stage was scanned for further analysis. Inside each well, the protectant liquid was removed and then 50 μL of MB solution was added for incubation at 25℃, 30 min. Finally, the bioluminescence of recovered BLN pieces was scanned to evaluate the frozen-thawed process.

1.9 The reuse of BLN

To investigate the robustness of the BLN device, a set of 6 sterile nanocellulose pieces were added into 25 mL of MB culture inoculated with 0.1% of inoculum at 25 ℃, 140 rpm. After cultivation of 18 h, BLN were scanned to measure the luminescence as the initial intensity. Then those BLN pieces were washed twice by 2% NaCl and sterilized at 121 ℃ for 20 min. The process was repeated by inoculating 25 μL of bacteria into 25 mL MB culture containing those

cooled nanopaper pieces and cultivating as a routine set. At the end of each cycle, the bioluminescence intensity was scanned and compared with the initial one for 10 cycles.

1.10 Data analysis

ImageJ 1.46r software was employed to analyze the bioassay pictures scanned by Typhoon. First, the scanning pictures were adjusted for better contrast by "*Image*" option (this process does not modify the original grayscale values of the images). To distinguish the bioassays from different contaminants, the color of each treatment was changed in ¨*Image*¨ and "*Lookup Tables*" option. Then the bioluminescence intensity was measured by ¨*Oval selection*¨ tool and calculated in grayscale.

To determine the EC_{50} of each toxicant, the observed concentration-response data were fitted to the modified non-linear equation (1) [28]:

$$I = \alpha + (\beta - \alpha)/(1 + 10^{((\log EC_{50} - \log C) * k)}) \quad (1)$$

where I is the luminescent intensity; α and β are the parameters of the models; EC_{50} is the concentration of test chemicals that provokes a response half way between the maximal (β) response and the maximally inhibited (α) response; C represents the test concentration of chemicals and k describes the steepness of the curve.

2. Results and Discussion

In marine ecosystem, the bioluminescence of *A. fischeri* was the outcome of the cell-to-cell communication. Once the bacteria reach to a high cell density, they switch on the ¨quorum sensing¨ mode and emit light [29-30]. In order to understand its growth cycle and luminescent emission, *A. fischeri* was inoculated and cultivated in liquid and agar cultures, respectively. Within 20 h, bacteria experienced the lag, exponential and stationary phases sequentially (Figure

1D). At 12 to 14 h, the bioluminescence in two cultures peaked at the highest intensity but decreased sharply afterwards, implying the instability of light emission in both systems (Figure 1E). Then *A. fischeri* at 2.3×10^{8} CFU mL^{-1} (calibrated in Figure S1) was inoculated on the round-shaped pieces of nanocellulose (5 mm of diameter) and underwent three physiological phases as normal (Figure 1D). Unlike the dramatic fluctuations in conventional cultures, the bioluminescence in BLN was more stable and persistent because of the biocompatible and flexible bio-support (Figure 1E). In smart phone pictures, the colour of BLN turned yellowish as its turbidity was higher than the transparent bare nanocellulose (see Figure 1A and 1B, left). By scanning, BLN sample showed intensive and homogenous luminescence emission (see Figure 1B, right). Meanwhile, the SEM images displayed that the network of nanocellulose remained as rich and crossed nets after immobilization but densely filled with bacteria (see Figure 1a and 1b). During the bacteria immobilization process, the quantity of bacteria was increased due to the proliferation of numerous cells. Some newly divided bacteria were trapped into the nanocellulose network. With their growing, the size of bacteria was enlarged in the life cycle, which spread the surrounding nanocellulose fibres and made the network pores bigger than those without bacteria. For example, in Fig.1 b, the background nanocellulose (without bacteria) demonstrated the same density as Fig.1 a (the bare nanopaper). Therefore, the difference in density showing in before- and after-immobilization process (Figure 1a and 1b) would be caused by the stretch of growing bacteria. Besides, this phenomenon also demonstrated the excellent flexibility of nanocelullose paper. Surprisingly, one bacterium was even undergoing the cell division process, proving the impressive biocompatibility of nanocellulose in *A. fischeri*'s metabolism (Figure S2D). Moreover, the three-dimensional (3D) confocal microscopy images of BLN illustrated the

intensive and homogenous distribution of *A. fischeri* onto/into the nanopaper structure, which in fact contributed to the strong light emission of BLN composite (Figure 1C, 1c and Movie S1).

Typically, suspension/adherent culture is used for cell enrichment that can efficiently provide a large number of cells. Based on new culture substrates and techniques, the 3D formation of cell communities has become a hot topic recently. Bacterial nanocellulose secreted by *Acetobacter xylinum* has showed up as one of those emerging materials for cell/tissue engineering of stem cells [24, 31], tumor [25] and cartilage [32-33]. As we first report here, bacterial nanocellulose has exhibited its outstanding biocompatibility with marine bacteria *A. fischeri*, which realized normal proliferation of bacteria on an abundant, low-cost substrate with stable genetic expression. Besides, the use of general luminescent equipment enabled a more rapid and simultaneous measurement of bioluminescence, leading to a bio-composite that operates as a simple-to-fabricate and user-friendly device in practical applications such as toxicity determination.

Environmental monitoring is a prevalent topic in the scientific field and the public areas, in which toxicity bioassays have been a widely-used mean for their significant importance to determine the biological impacts of known/unknown pollutants on living organisms. Commercially, Microtox® has been recommended as a standard tool to reveal the toxic level of sole/complex toxin(s) towards aquatic environment in the last decades [6]. In this study, the toxicity levels of diuron, TBT and PBDE was classified by Microtox® (Table S1, Figure S3), showing that *A. fischeri* was highly sensitive to these three xenobiotics. In Microtox® kit, the bio-reagent *A. fischeri* is prepared as a freeze-dried powder with high uniformity for toxicity evaluation and typically stored at low temperature (-20 ℃). Since its high price and unique measurement, the kit may lack the ability of large-scale screening in practice. Nevertheless, using immobilized bacteria may facilitate a low-cost and simple-to-fabricate bioassay platform.

Hence, we investigated the toxicity assays of three compounds via *A. fischeri*-decorated BLN. As displayed in Figure 2, the optical intensity of each treatment decreased gradually with the decrease of toxic concentrations, which fitted well in the symmetrical sigmoidal curves (see also Figure S5). By calculation, the EC_{50} of diuron, TBT and PBDE were 108.2 mg L^{-1}, 0.24 mg L^{-1} and 8.7 μg L^{-1}, respectively. Comparing to those results from Microtox® and free-cell evaluation (Figure S3 and S4), the use of BLN showed comparable analytical behavior and accuracy (Table S1). To be specific, higher EC_{50} values were obtained from free-cell tests (123 mg L^{-1}, 0.46 mg L^{-1} and 11.6 μg L^{-1}, respectively), which indicated that bacteria-immobilized BLN devices were more sensitive than free-cell suspension. In comparison to standard Microtox® tests, similar performance was obtained as the EC_{50} of TBT and PBDE were 0.27 mg L^{-1} and 15.8 μg L^{-1} using Microtox® (that was 0.24 mg L^{-1} and 8.7 μg L^{-1} via BLN). Different from TBT and PBDE tests, less sensitive performance was observed in diuron as the EC_{50} was 21.1 mg L^{-1} by Microtox® whilst 108.2 mg L^{-1} via BLN. According to reported studies, however, the EC_{50} value of diuron varied significantly from 8 to 86 mg L^{-1} (Table S2), which might imply that different batches of bio-reagent *A. fischeri* or operation conditions might have an effect on the bioassay sensitivity, leading to the distinct toxicity levels of diuron. In the present work, the luminescence inhibition induced by diuron in BLN could be fitted in the statistic model with predictable EC_{50} level, which confirmed its possibility for further study. As expected, *A. fischeri* retained its sensitivity to xenobiotics in the form of BLN devices. Taking the advantage of the simple fabrication and easy operation, the proposed nanobiocomposite facilitates a rapid, sensitive, non-invasive and broadly available platform for the evaluation of various toxicants.

The applicability to real samples is regarded as the ultimate goal for a bioassay platform. In this context, simplification of the test process and avoiding secondary pollution coming from the

test itself is highly desired. The proposed BLN device was expected to function with environmental samples so as to demonstrate its accessibility for practical applications. Consequently, we estimated its sensitivity in both lake water and seawater, whose no adverse effect on BLN luminescence properties was previously confirmed (see Figure S6 and S7). The inhibition of bacterial luminescence by exposing to toxic compounds for 5 and 15 min was measured and plotted in Figure 3. In real matrixes, BLN devices kept stable and higher sensitivity towards TBT in spiked lake water or sea water. Comparing the EC_{50} to those samples analyzed in pure water, the EC_{50} of TBT was 0.27 mg L^{-1} in lake water and even lower at 0.18 mg L^{-1} in spiked sea water (that was 0.24 mg L^{-1} in pure water test). However, the sensitivity of BLN composites decreased towards diuron and PBDE (Table S3). Particularly, the EC_{50} of PBDE increased dramatically to approximately 30 μg L^{-1} in spiked real matrixes compared to 8.7 μg L^{-1} in pure water. The matrix effect could possibly be a major reason for the lower sensitivity of BNL devices in real samples. Bacteria *A. fischeri* was discovered and isolated from a marine creature. In the laboratory incubation, bacteria cells also require the high salinity culture to proliferate and emit bioluminescence. In the real matrix, especially the sea water, the matrix may contain complex ingredients or trace elements that provided *A. fischeri* a suitable environment as buffer, which could enhance its resistance against toxic xenobiotics, leading to lower sensitivity. In addition, the toxic agents at low concentrations demonstrate stimulatory effects to living organisms, which was generally observed and described as hormesis effect [34-35]. Since the low concentration of PBDE (at 0.2 mg L^{-1}) was spiked in lake and sea water, the less sensitive performance of *A. fischeri*-decorated BLN in real matrix could be a result of the low-dose stimulation relationship phenomenon.

According to these results, BLN platform exhibited many advantages in the application of toxicity bioassay. First, the BLN device was simple to fabricate based on cheap and abundant ingredients. Bacteria-derived nanocellulose as cell culture skeleton was a sustainable biomaterial with high permeability, flexibility and great biocompatibility to luminescent marine bacteria *A. fischeri*. These inherent properties of nanocellulose enabled BLN to be a low-cost, controllable and easy-to-assembly bio-composite representing no threat to the environment. After bacteria immobilization, the biological character of *A. fischeri* was retained in the BLN architecture, keeping its stable and persistent bioluminescence emission in toxicity screening. Second, sensitivity is the primary rule for toxicity screening. BLN platform demonstrated a high sensitivity towards hazardous compounds that is comparable with the gold standard of this kind of bioassays. More importantly, BLN demonstrated its broad applicability with real matrix, which highlighted its potential for the practical *in-situ* use with shortened and simplified process. In addition, the bioluminescence intensity of BLN setup could be measured by a one-step simultaneous scan with a general scanner or a microplate reader instead of a special luminescence analyzer. No particular expertise or skills is required during the bioassay process, which allowed the wide use of BLN platform for practical needs. Overall, the fabrication of BLN based on nanocellulose as a bio-support and *A. fischeri* as a bio-indicator may facilitate a rapid, sensitive, low-cost, controllable and non-invasive toxicity bioassay with general and portable equipment. Since *A. fischeri* exhibited its broad sensitivity to thousands of chemicals, BLN device is amenable to being applied as a broadly accessible platform for toxicity screening of xenobiotic complexes under *in-situ* conditions.

Storability and reusability may endow the present BLN platform with more competitive advantages for the further large-scale fabrication and commercial application. Consequently, we

also investigated the performance of BLN after frozen-thawed process and recycling process, respectively. In general, the frozen-thawed process was conducted under the protection of cryoprotective agents including polyalcohol, amino acids and disaccharides [36-38]. As showing in Figure 4, we investigated the recovered bioluminescence of BLN devices frozen with glycine/sucrose/glycerol at -20 ℃. Due to the potential toxicity of cryoprotectants, the bioluminescence of BLN slightly decreased after adding those protective agents. The group treated with glycine indicated the best preservation of bioluminescence since more than 60% of the bioluminescent intensity regained by applying 5%, 10% and 15% of glycine. Particularly, the luminescence of BLN devices under the protection of 5% of glycine resumed to approximate 80% of the initial intensity, even surpassing the luminescent level before freezing, which suggested that BLN could tolerate the freezing storage with 5% of glycine. Thus, we employed those frozen-thawed BLN devices (in 5% of glycine) to perform a toxicity assay using diuron as a model pollutant. In Figure 4D, the frozen-thawed BLN could estimate the toxic level of diuron (EC_{50} at 195.6 mg L^{-1}) (that is 108.2 mg L^{-1} compared to that from the unfrozen platform). Although the frozen-thawed device showed lower sensitivity than unfrozen platform, it still indicated that BLN composites had the potential to remain the bio-function in toxicity bioassay through cryopreservation process. In a future study, optimization on freezing process would be required to improve the survival of *A. fischeri* and the sensitivity of frozen BLN devices, for instance, using lyophilisation technique.

Next, we evaluated the reusability of BLN devices by recycling used BLN and repeating the bacteria immobilization process. Figure 4E illustrates the stable intensity of BLN luminescence after 10 cycles, implying the great robustness of BLN composites and their biocompatibility to bacteria *A. fischeri* was retained after recycling. Taking the benefit of its reusability, these robust

BLN devices not only realized a green and low-cost fabrication, but also might have great potential for an automatically assembling setup, like wiping and reloading luminescent bacteria after use. Herein, the BLN device presented its properties as a novel, robust and green platform for toxicity assays, highlighting its unique potential in large-scale fabrication and ready-to-use application by frozen-thawed preservation.

3. Conclusions

We have demonstrated a low-cost, green, controllable and simple-to-fabricate BLN device based on bacterial nanocellulose as both a culture scaffold and biosensing substrate and luminescent bacteria *A. fischeri* as a bio-indicator. By determining the luminescent inhibition caused by the exposure of toxicants, the novel BLN platform operated as an efficient and sensitive platform for fast toxicity screening of various xenobiotics. Moreover, BLN devices indicated broad applicability upon environmental samples, which enabled the direct and *in-situ* assessment. More importantly, the BLN setup has facilitated a one-step and user-friendly measurement with general analyzer, highlighting its potential for environmental monitoring through a simplified process. Finally, our BLN architecture has exhibited good tolerance during freezing storage as well as great robustness in recycling process, which may endow the BLN system with competitive advantages as a deliverable, ready-to-use device in the large-scale manufacture, even with the potential of being an automatically assembling portable device.

Figures

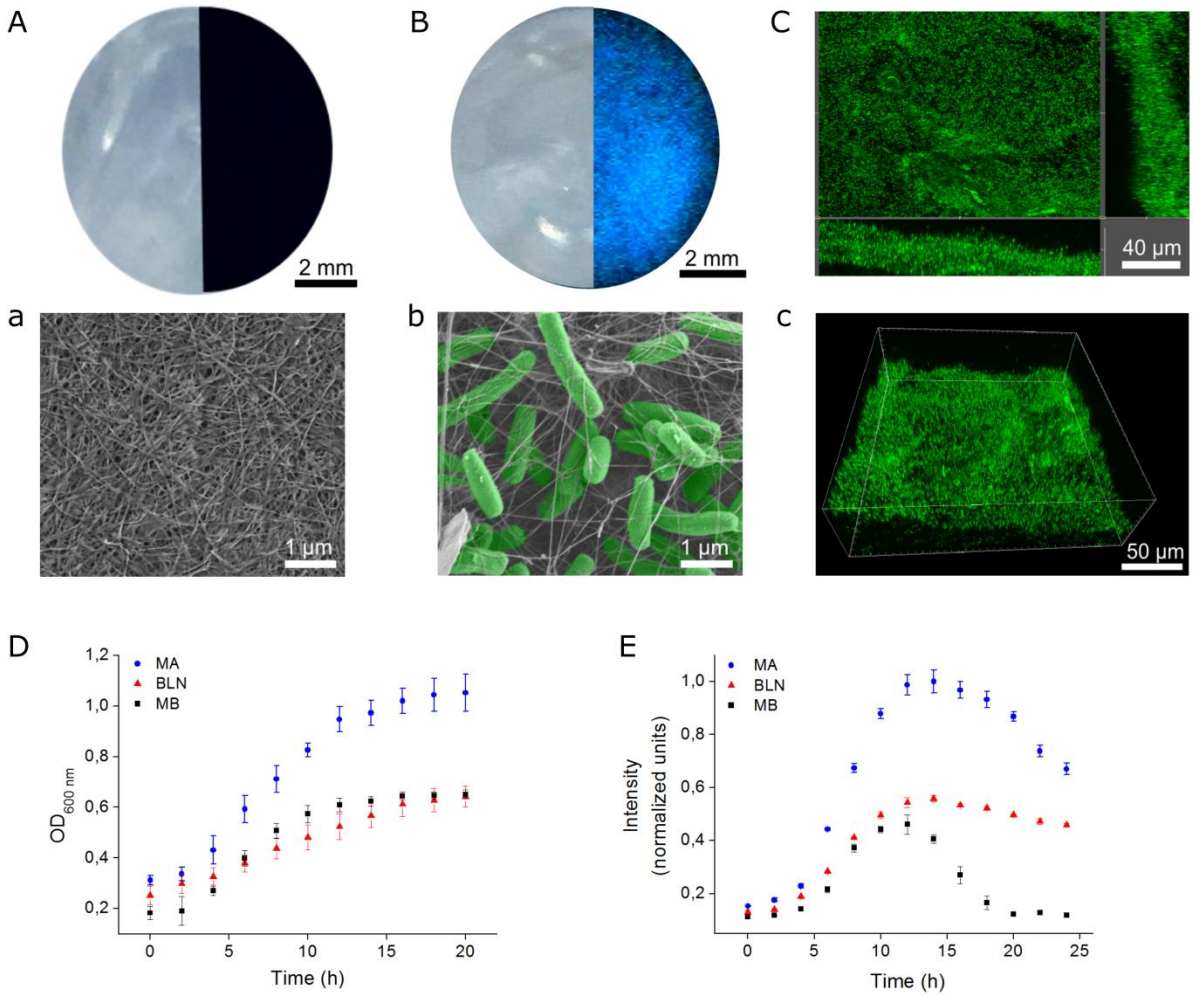

Figure 1. The characterization of *A. fischeri*–decorated BLN platform. (A) Physical appearance of bare nanocellulose by smart phone (left) and its scanned image (right). (a) Scanning electron microscopy (SEM) micrograph of bare bacterial nanocellulose. (B) Physical appearance of *A. fischeri*-decorated BLN by smart phone (left) and its scanned image (right). (b) SEM micrograph

of BLN. (C-c) Confocal microscopy images of BLN. (C) Top view and cross-section. (c) 3d view. (D) The growth tendency. (E) The trend of bioluminescence intensity across time.

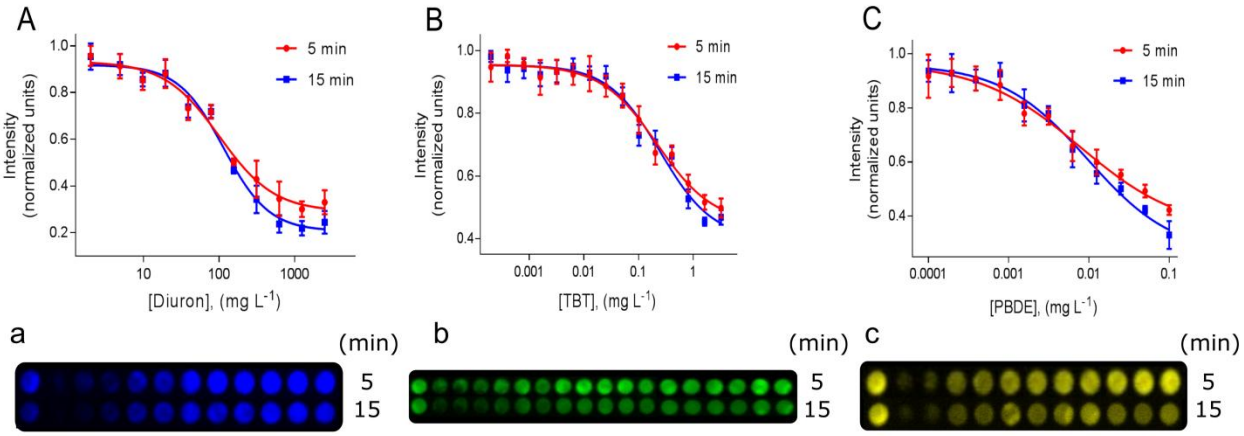

Figure 2. The bioluminescence inhibition in *A. fischeri*–decorated BLN devices via toxic dilutions exposure. (A) The calibration curve related to diuron and (a) the scanned image showing the corresponding bioluminescence. (B) The calibration curve related to TBT and (b) the corresponding scanned image. (C) The calibration curve related to PBDE and (c) the corresponding scanned image. (a-c) Experimental examples.

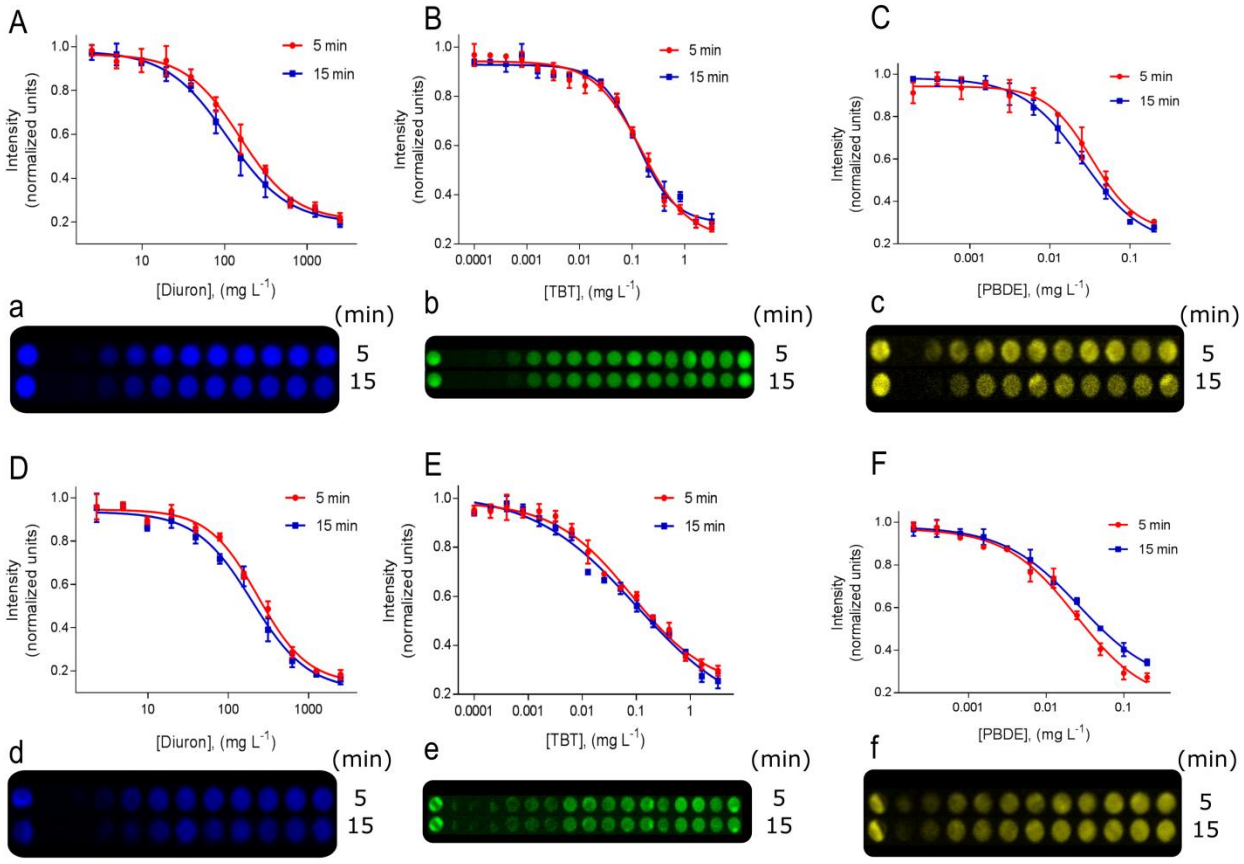

Figure 3. The bioluminescence inhibition in *A. fischeri*-decorated BLN by toxic-spiked real matrix. (A-C) Analysis in spiked lake water. The calibration curves of (A) diuron, (B) TBT and (C) PBDE and the corresponding scanned images of (a) diuron, (b) TBT and (c) PBDE. (D-F) The calibration curves and (d-f) experimental examples of BLN in spiked seawater.

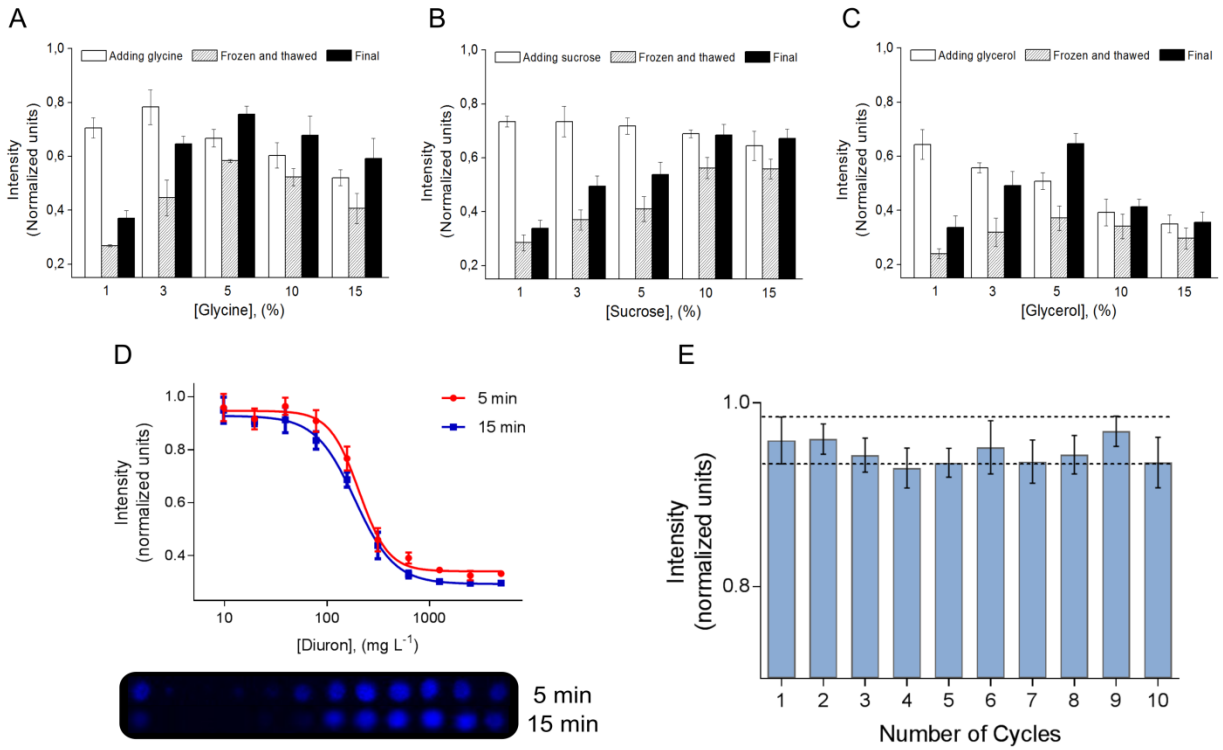

Figure 4. BLN after frozen-thawed process. Frozen with (A) glycine; (B) sucrose and (C) glycerol. (D) Bioassay of diuron with the frozen-thawed BLN composites. (E) The bioluminescence of recycled BLN

Scheme

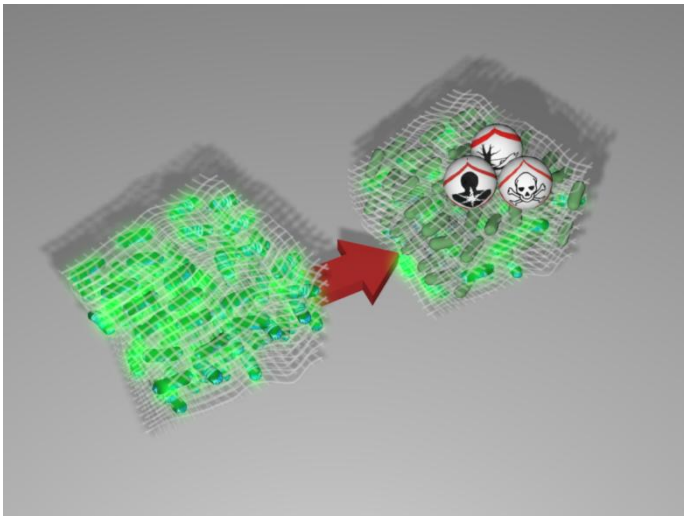

Scheme 1. Schematic the proposed nanopaper-based bioassay

Acknowledgements

This work was supported by the European Commission Program, H2020-WATER, INTCATCH Project (689341). ICN2 acknowledges support from the Severo Ochoa Program (MINECO, Grant SEV-2013-0295). The Nanobiosensors and Bioelectronics Group acknowledges the support from the Generalitat de Cataluña (Grant 2014 SGR 260). Jie Liu acknowledges the support from China Scholarship Council (CSC).

References

[1] Sturm, S.; Hammann, F.; Drewe, J.; Maurer, H. H.; Scholer, A., An automated screening method for drugs and toxic compounds in human serum and urine using liquid chromatography–tandem mass spectrometry. *J. Chromatogr. B* **2010,** *878* (28), 2726-2732.

[2] Maurer, H. H., What is the future of (ultra) high performance liquid chromatography coupled to low and high resolution mass spectrometry for toxicological drug screening? *J. Chromatogr. A* **2013,** *1292*, 19-24.

[3] Blasco, C.; Picó, Y., Prospects for combining chemical and biological methods for integrated environmental assessment. *TrAC Trend Anal. Chem.* **2009,** *28* (6), 745-757.

[4] Yu, D.; Liu, J.; Sui, Q.; Wei, Y., Biogas-pH automation control strategy for optimizing organic loading rate of anaerobic membrane bioreactor treating high COD wastewater. *Bioresource Technol.* **2016,** *203*, 62-70.

467 [5] Oller, I.; Malato, S.; Sánchez-Pérez, J. A., Combination of Advanced Oxidation
468 Processes and biological treatments for wastewater decontamination—A review. *Sci. Total*
469 *Environ.* **2011,** *409* (20), 4141-4166.
470 [6] Parvez, S.; Venkataraman, C.; Mukherji, S., A review on advantages of implementing
471 luminescence inhibition test (Vibrio fischeri) for acute toxicity prediction of chemicals. *Environ.*
472 *Int.* **2006,** *32* (2), 265-268.
473 [7] Rizzo, L., Bioassays as a tool for evaluating advanced oxidation processes in water and
474 wastewater treatment. *Water Res.* **2011,** *45* (15), 4311-4340.
475 [8] Farré, M.; Barceló, D., Toxicity testing of wastewater and sewage sludge by biosensors,
476 bioassays and chemical analysis. *TrAC Trend Anal. Chem.* **2003,** *22* (5), 299-310.
477 [9] Ma, X. Y.; Wang, X. C.; Ngo, H. H.; Guo, W.; Wu, M. N.; Wang, N., Bioassay based
478 luminescent bacteria: Interferences, improvements, and applications. *Sci. Total Environ.* **2014,**
479 *468–469*, 1-11.
480 [10] Xiao, Y.; Araujo, C. D.; Sze, C. C.; Stuckey, D. C., Toxicity measurement in biological
481 wastewater treatment processes: A review. *J. Hazard. Mater.* **2015,** *286*, 15-29.
482 [11] Wieczerzak, M.; Namieśnik, J.; Kudłak, B., Bioassays as one of the Green Chemistry
483 tools for assessing environmental quality: A review. *Environ. Int.* **2016,** *94*, 341-361.
484 [12] Hsieh, C.-Y.; Tsai, M.-H.; Ryan, D. K.; Pancorbo, O. C., Toxicity of the 13 priority
485 pollutant metals to Vibrio fisheri in the Microtox® chronic toxicity test. *Sci. Total Environ.* **2004,**
486 *320* (1), 37-50.
487 [13] Joly, P.; Bonnemoy, F.; Charvy, J.-C.; Bohatier, J.; Mallet, C., Toxicity assessment of the
488 maize herbicides S-metolachlor, benoxacor, mesotrione and nicosulfuron, and their

corresponding commercial formulations, alone and in mixtures, using the Microtox® test. *Chemosphere* **2013,** *93* (10), 2444-2450.

[14] Kralj, M. B.; Trebše, P.; Franko, M., Applications of bioanalytical techniques in evaluating advanced oxidation processes in pesticide degradation. *TrAC Trend Anal. Chem.* **2007,** *26* (11), 1020-1031.

[15] Isidori, M.; Lavorgna, M.; Nardelli, A.; Pascarella, L.; Parrella, A., Toxic and genotoxic evaluation of six antibiotics on non-target organisms. *Sci. Total Environ.* **2005,** *346* (1–3), 87-98.

[16] van der Grinten, E.; Pikkemaat, M. G.; van den Brandhof, E.-J.; Stroomberg, G. J.; Kraak, M. H. S., Comparing the sensitivity of algal, cyanobacterial and bacterial bioassays to different groups of antibiotics. *Chemosphere* **2010,** *80* (1), 1-6.

[17] Journal of Chromatography BHeidari, F.; Asadollahi, M. A.; Jeihanipour, A.; Kheyrandish, M.; Rismani-Yazdi, H.; Karimi, K., Biobutanol production using unhydrolyzed waste acorn as a novel substrate. *RSC Adv.* **2016,** *6* (11), 9254-9260.

[18] Chang, Z.; Cai, D.; Wang, Y.; Chen, C.; Fu, C.; Wang, G.; Qin, P.; Wang, Z.; Tan, T., Effective multiple stages continuous acetone–butanol–ethanol fermentation by immobilized bioreactors: Making full use of fresh corn stalk. *Bioresource Technol.* **2016,** *205*, 82-89.

[19] Tang, Y.; Werth, C. J.; Sanford, R. A.; Singh, R.; Michelson, K.; Nobu, M.; Liu, W.-T.; Valocchi, A. J., Immobilization of Selenite via Two Parallel Pathways during In Situ Bioremediation. *Environ. Sci. Technol.* **2015,** *49* (7), 4543-4550.

[20] Liu, J.; Chen, S.; Ding, J.; Xiao, Y.; Han, H.; Zhong, G., Sugarcane bagasse as support for immobilization of Bacillus pumilus HZ-2 and its use in bioremediation of mesotrione-contaminated soils. *Appl. Microbiol. Biot.* **2015,** *99* (24), 10839-10851.

[21] Morales-Narváez, E.; Golmohammadi, H.; Naghdi, T.; Yousefi, H.; Kostiv, U.; Horák, D.; Pourreza, N.; Merkoçi, A., Nanopaper as an Optical Sensing Platform. *ACS Nano* **2015,** *9* (7), 7296-7305.

[22] Klemm, D.; Kramer, F.; Moritz, S.; Lindström, T.; Ankerfors, M.; Gray, D.; Dorris, A., Nanocelluloses: A New Family of Nature-Based Materials. *Angew. Chem. Int. Edit.* **2011,** *50* (24), 5438-5466.

[23] Heli, B.; Morales-Narvaez, E.; Golmohammadi, H.; Ajji, A.; Merkoci, A., Modulation of population density and size of silver nanoparticles embedded in bacterial cellulose via ammonia exposure: visual detection of volatile compounds in a piece of plasmonic nanopaper. *Nanoscale* **2016,** *8* (15), 7984-7991.

[24] Mertaniemi, H.; Escobedo-Lucea, C.; Sanz-Garcia, A.; Gandía, C.; Mäkitie, A.; Partanen, J.; Ikkala, O.; Yliperttula, M., Human stem cell decorated nanocellulose threads for biomedical applications. *Biomaterials* **2016,** *82*, 208-220.

[25] Xiong, G.; Luo, H.; Zhu, Y.; Raman, S.; Wan, Y., Creation of macropores in three-dimensional bacterial cellulose scaffold for potential cancer cell culture. *Carbohyd. Polym.* **2014,** *114*, 553-557.

[26] Bose, J. L.; Kim, U.; Bartkowski, W.; Gunsalus, R. P.; Overley, A. M.; Lyell, N. L.; Visick, K. L.; Stabb, E. V., Bioluminescence in Vibrio fischeri is controlled by the redox-responsive regulator ArcA. *Mol. Microbiol.* **2007,** *65* (2), 538-553.

[27] de la Escosura-Muñiz, A.; Chunglok, W.; Surareungchai, W.; Merkoçi, A., Nanochannels for diagnostic of thrombin-related diseases in human blood. *Biosens. Bioelectro.* **2013,** *40* (1), 24-31.

[28] Villa, S.; Vighi, M.; Finizio, A., Experimental and predicted acute toxicity of antibacterial compounds and their mixtures using the luminescent bacterium Vibrio fischeri. *Chemosphere* **2014,** *108*, 239-244.

[29] Galloway, W. R. J. D.; Hodgkinson, J. T.; Bowden, S. D.; Welch, M.; Spring, D. R., Quorum Sensing in Gram-Negative Bacteria: Small-Molecule Modulation of AHL and AI-2 Quorum Sensing Pathways. *Chem. Rev.* **2011,** *111* (1), 28-67.

[30] Ng, W.-L.; Bassler, B. L., Bacterial Quorum-Sensing Network Architectures. *Annu. Rev. Genet.* **2009,** *43*, 197-222.

[31] L. Cacicedo, M.; E. León, I.; S. Gonzalez, J.; M. Porto, L.; A. Alvarez, V.; Castro, G. R., Modified bacterial cellulose scaffolds for localized doxorubicin release in human colorectal HT-29 cells. *Colloid. Surface. B* **2016,** *140*, 421-429.

[32] Ah S SensFavi, P. M.; Ospina, S. P.; Kachole, M.; Gao, M.; Atehortua, L.; Webster, T. J., Preparation and characterization of biodegradable nano hydroxyapatite–bacterial cellulose composites with well-defined honeycomb pore arrays for bone tissue engineering applications. *Cellulose* **2016,** *23* (2), 1263-1282.

[33] Svensson, A.; Nicklasson, E.; Harrah, T.; Panilaitis, B.; Kaplan, D. L.; Brittberg, M.; Gatenholm, P., Bacterial cellulose as a potential scaffold for tissue engineering of cartilage. *Biomaterials* **2005,** *26* (4), 419-431.

[34] Stebbing, A. R. D., Hormesis — The stimulation of growth by low levels of inhibitors. *Sci. Total Environ.* **1982,** *22* (3), 213-234.

[35] Calabrese, E. J.; Baldwin, L. A., Hormesis: the dose-response revolution. *Annu. Rev. Pharmacol.Toxicol.* **2003,** *43* (1), 175-197.

555 [36] Donnez, J.; Martinez-Madrid, B.; Jadoul, P.; Van Langendonckt, A.; Demylle, D.;
556 Dolmans, M.-M., Ovarian tissue cryopreservation and transplantation: a review. *Hum. Reprod. Update* **2006,** *12* (5), 519-535.
557
558 [37] Kovalevsky, G.; Carney, S. M.; Morrison, L. S.; Boylan, C. F.; Neithardt, A. B.; Feinberg,
559 R. F., Should embryos developing to blastocysts on day 7 be cryopreserved and transferred:
560 an analysis of pregnancy and implantation rates. *Fertil. Steril.* **2013,** *100* (4), 1008-1012.
561 [38] Subbarayan, K.; Rolletschek, H.; Senula, A.; Ulagappan, K.; Hajirezaei, M.-R.; Keller, E.
562 R. J., Influence of oxygen deficiency and the role of specific amino acids in cryopreservation of
563 garlic shoot tips. *BMC Biotechnol.* **2015,** *15* (1), 40.

564